Available online at www.sciencedirect.com
ScienceDirect
Trans. Nonferrous Met. Soc. China 31(2021) 3469−3477
Transactions of Nonferrous Metals Society of China
www.tnmsc.cn

# Mn nanoparticles enhanced dehydrogenation and hydrogenation kinetics of $MgH_2$ for hydrogen storage

Yan CHEN[1], Hao-yu ZHANG[1], Fu-ying WU[2], Ze SUN[1], Jia-guang ZHENG[1], Liu-ting ZHANG[1], Li-xin CHEN[3]

1. School of Energy and Power, Jiangsu University of Science and Technology, Zhenjiang 212003, China;
2. Analysis and Testing Center, Jiangsu University of Science and Technology, Zhenjiang 212003, China;
3. State Key Laboratory of Silicon Materials, Department of Materials Science and Engineering, Zhejiang University, Hangzhou 310027, China

Received 30 August 2021; accepted 10 November 2021

**Abstract:** Mn nanoparticles (nano-Mn) were successfully synthesized and doped into $MgH_2$ to improve its de/hydrogenation properties. Compared with $MgH_2$, the onset desorption temperature of 10 wt.% nano-Mn modified $MgH_2$ was decreased to 175 °C and 6.7, 6.5 and 6.1 wt.% hydrogen could be released within 5, 10 and 25 min at 300, 275 and 250 °C, respectively. Besides, the composite started to take up hydrogen at room temperature and absorbed 2.0 wt.% hydrogen within 30 min at low temperature of 50 °C. The hydrogenation activation energy of $MgH_2$ was reduced from (72.5±2.7) to (18.8±0.2) kJ/mol after doping with 10 wt.% nano-Mn. In addition, the $MgH_2$ + 10 wt.% nano-Mn composite exhibited superior cyclic property, maintaining 92% initial capacity after 20 cycles.
**Key words:** hydrogen storage material; magnesium hydride; Mn nanoparticles; catalytic mechanism; reversibility

## 1 Introduction

Hydrogen energy, which has a high energy density of 142 MJ/kg and produces only clean and non-toxic water after combustion, is considered to be one of the most promising renewable energies to mitigate global energy crisis and achieve a carbon-neutral society [1−3]. Nevertheless, the practical application of hydrogen energy confronts many technological barriers, especially a safe and efficient hydrogen storage technology [1,4]. Compared with liquid hydrogen storage at cryogenic temperature (−253 °C, 0.5−1 MPa) and gaseous hydrogen storage limited by high pressure (35−70 MPa at room temperature), hydrogen stored in solid-state materials not only has the advantage of high hydrogen storage density, but also can ensure safety in the process of utilization [5−8].

$MgH_2$, which has the characteristics of high gravimetric (7.6 wt.%) and volumetric (110 kg/m$^3$) hydrogen capacity, low cost and excellent reversibility, is promising to meet the requirements of practical hydrogen storage application [9−14]. Unfortunately, high thermodynamic stability and poor kinetic property of $MgH_2$ impede its practical application [15−17]. In order to overcome the above-mentioned problems, various strategies have been carried out in the past few decades such as nano-structuring [18−21], alloying [22−25] and catalyst doping [26−30]. Among them, transition metal related additives are proven to greatly facilitate the hydrogen storage property of $MgH_2$ [31−36]. For example, LIANG et al [37] investigated 5 wt.% TMs (Ti, V, Mn, Fe, and Ni) modified $MgH_2$ and found V and Ti showed superior catalytic effect on de/rehydrogenation properties of $MgH_2$. By decreasing the particle size

**Corresponding author:** Liu-ting ZHANG, Tel: +86-15262913186, E-mail: zhanglt89@just.edu.cn
DOI: 10.1016/S1003-6326(21)65743-6

of the catalyst, the catalytic effect towards the hydrogen storage property of $MgH_2$ could be further improved. ZHANG et al [38] and MA et al [39] found that nano-sized $TiH_{1.971}$ and Ni-doped $MgH_2$ quickly released over 6.0 wt.% hydrogen at 300 °C, while pristine $MgH_2$ released almost no hydrogen under the same condition. PATELLI et al [40] successfully synthesized Mg−Ti−H nanoparticles and the reversible absorption of hydrogen within $MgH_2$−Mg phase transition was achieved in a remarkably low temperature range of 65−150 °C.

Besides above regularly investigated transition metals, Mn related catalysts were also demonstrated effective for $MgH_2$. In our previous study [41], the $MgH_2$ + 10 wt.% nano-$ZrMn_2$ composite released 6.7 wt.% hydrogen in 5 min at 300 °C. DFT calculation denoted that $ZrMn_2$ reduced the strength of Mg—H bond and lowered the dehydrogenation and hydrogenation temperature. Later, Mn-based catalysts ($MnCl_2$ and submicron-Mn) were doped into $MgH_2$ to enhance the hydrogen storage property [42]. The thermogravimetry tests showed that onset dehydrogenation temperatures of $MnCl_2$ and submicron-Mn doped $MgH_2$ could be reduced to 225 and 183 °C while the undoped $MgH_2$ started to release hydrogen at 315 °C. Nanoscale catalyst can provide more active sites and nucleation centers for hydrogen absorption and desorption, and thus can effectively improve the kinetic performance of $MgH_2$ [43,44]. However, as far as we know, no report has been published about the direct use of nano-sized Mn on enhancing the hydrogen storage property of $MgH_2$. Thus, Mn nanoparticles (20−30 nm) were successfully synthesized to further investigate the particle size effect on the catalytic action on $MgH_2$ in this work.

## 2 Experimental

### 2.1 Sample preparation

2.1.1 Preparation of $MgH_2$

The $MgH_2$ powders were prepared by hydrogenation heat treatment and mechanical ball milling. Primarily, the commercial Mg powders were hydrogenated in a Sieverts-type volumetric apparatus at 380 °C and hydrogen pressure of 6.5 MPa for 2 h. Afterwards, the samples were ball-milled at a speed of 450 r/min for 5 h with a ball-to-powder mass ratio of 40:1 in a planetary ball mill system (QM-3SP4, Nanjing Chishun, China). The above steps were repeated twice and $MgH_2$ could be finally obtained.

2.1.2 Preparation of Mn nanoparticles

Mn nanoparticles were prepared by mechanical ball milling, commercially available $MnCl_2$, (98%, Sinopharm Chemical Reagent Co., Shanghai, China), LiCl (99%, Aladdin Biochemical Technology Co., Shanghai, China) and LiH (97%, Aladdin Biochemical Technology Co., Shanghai, China). In brief, the mixture of 1 g $MnCl_2$ and 0.5 g LiCl were pre-milled for 2 h by using a mechanical ball mill at a speed of 400 r/min. Subsequently, 0.32 g LiH was added to the mixture and milled for 20 h. To make the raw materials react completely and prevent them from clumping, the mixture was tamped every 5 h. Anhydrous tetrahydrofuran was utilized to wash the mixture for 16−20 times to remove LiCl. Finally, Mn nanoparticles could be obtained after being vacuumed at room temperature for 12 h, denoted as nano-Mn.

2.1.3 Preparation of $MgH_2$ + nano-Mn composites

The above-synthesized Mn nanoparticles and $MgH_2$ were mixed at a mass ratio of 5:95, 10:90, 15:85 and then ball milled for 2 h at the speed of 450 r/min with a ball-to-material mass ratio of 40:1. Three composites were labeled as $MgH_2$ + 5 wt.% nano-Mn, $MgH_2$ + 10 wt.% nano-Mn and $MgH_2$ + 15 wt.% nano-Mn, respectively.

### 2.2 Sample characterization

An X'Pert Pro X-ray diffractometer with Cu $K_\alpha$ radiation ($\lambda$=0.15405 nm, 40 kV, 15 mA) was applied to exploring the phase structure and the composition of samples from 10° to 80° ($2\theta$) with a scanning speed of 5 (°)/min and 0.02 (°)/step. In addition, the morphology of the samples was characterized by transmission electron microscope (TEM, Tecnai G2 F30 S-TWIN) with energy dispersive X-ray spectrometer (EDS).

Non/-isothermal de/hydrogenation properties of the prepared compositions were studied by using a self-made Sievert-type apparatus. About 160 mg of samples were loaded in a reactor with temperature and pressure sensors and then were connected to the Sievert-type apparatus. During the non-isothermal dehydrogenation measurement, the reactor was heated from room temperature to 500 °C at a heating speed of 5 °C/min. For isothermal dehydrogenation measurement, the

reactor was prefilled with hydrogen (2.5 MPa) to prevent decomposition of samples during heating. Non-isothermal hydrogenation experiments were implemented from room temperature to 400 °C at a heating speed of 2 °C/min under hydrogen pressure of 3.2 MPa. In the isothermal hydrogenation examination, the whole hydrogenation system was heated to the preset temperature, and the data acquisition device would record the changes of temperature and pressure. Moreover, all operations and transfers were handled in a MIKROUNA glove box filled with Ar.

## 3 Results and discussion

### 3.1 Characterization of as-prepared Mn nanoparticles

During the preparation process, LiCl particles were utilized as nano-separators to prevent Mn particles from growing. To determine the micro-structure of synthesized Mn particles, X-ray diffraction (XRD) was performed. Figure 1(a) shows the XRD pattern of the as-synthesized Mn particles. According to the XRD result, the diffraction pattern matched well with the PDF# 32-0637 card of Mn and no other phases were detected. To explore the morphology and size of Mn particles, TEM observation was adopted. Figures 1(b, c) show TEM images of synthesized Mn under different magnifications. Clearly, the Mn particles were granular and homogeneously distributed. Based on TEM images, the average size of the catalyst was 20−30 nm, which proved that the catalyst prepared is nano-Mn.

### 3.2 Effect of Mn nanoparticles on hydrogen absorption and desorption properties of $MgH_2$

To investigate the catalytic effect of nano-Mn on $MgH_2$, temperature programed dehydrogenation (TPD) measurements were applied. Figure 2(a) shows the non-isothermal dehydrogenation curves of additive-free $MgH_2$, commercially available Mn and as-prepared nano-Mn modified $MgH_2$. For comparison, the non-isothermal dehydrogenation curve of submicron-Mn modified $MgH_2$ was also compiled [42]. As revealed in Fig. 2(a), additive-free $MgH_2$ began to dehydrogenate at 355 °C and ended at 400 °C with a capacity of 7.4 wt.%. The initial dehydrogenation temperature of the composite doped with 5 wt.% Mn decreased to 235 °C, and the dehydrogenation rate was similar to that of additive-free $MgH_2$. When the size of the doped catalyst is on micron level, the initial dehydrogenation temperature of the composite decreased significantly. It could be seen from Fig. 2(a) that $MgH_2$ + 5 wt.% submicron Mn released hydrogen from 183 °C, and 6.9 wt.% hydrogen could be released when the temperature was 375 °C. Compared with the $MgH_2$ + 5 wt.% submicron Mn composite, initial dehydrogenation temperature of $MgH_2$ + 5 wt.% nano-Mn was almost the same as that of $MgH_2$ + 5 wt.% nano-Mn composite, but the dehydrogenation rate was much faster. The dehydrogenation of $MgH_2$ + 5 wt.% nano-Mn composite ended at 315 °C, which was about 40 °C lower than that of $MgH_2$ + 5 wt.% submicron Mn composite.

Based on above results, it can be concluded that the catalytic effect of Mn increased with decreasing size. In order to determine the best doping amount of nano-Mn, 5, 10 and 15 wt.% doping amounts were selected as the contrast. Figures 2(b) shows that the onset dehydrogenation temperature of $MgH_2$ + 10 wt.% nano-Mn was 175 °C, about 8 °C lower than that of $MgH_2$ + 5 wt.% nano-Mn. Although the initial dehydrogenation temperature was further decreased when the doping

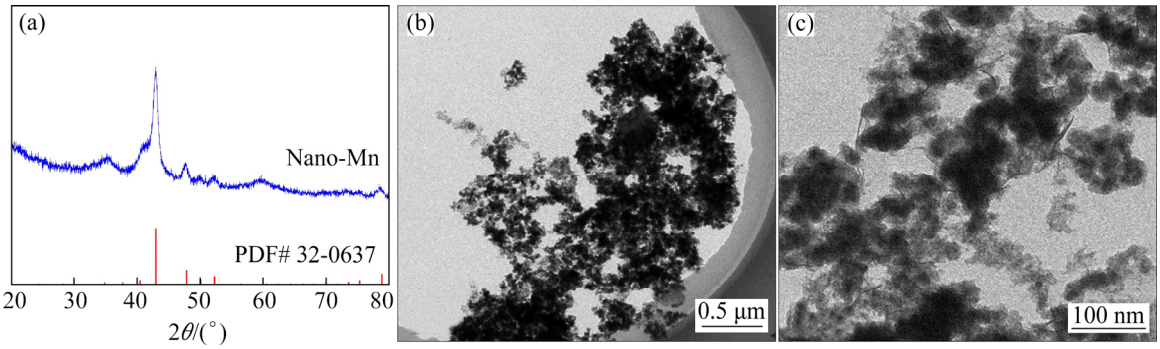


**Fig. 1** XRD pattern (a) and TEM images (b, c) of synthesized Mn particles

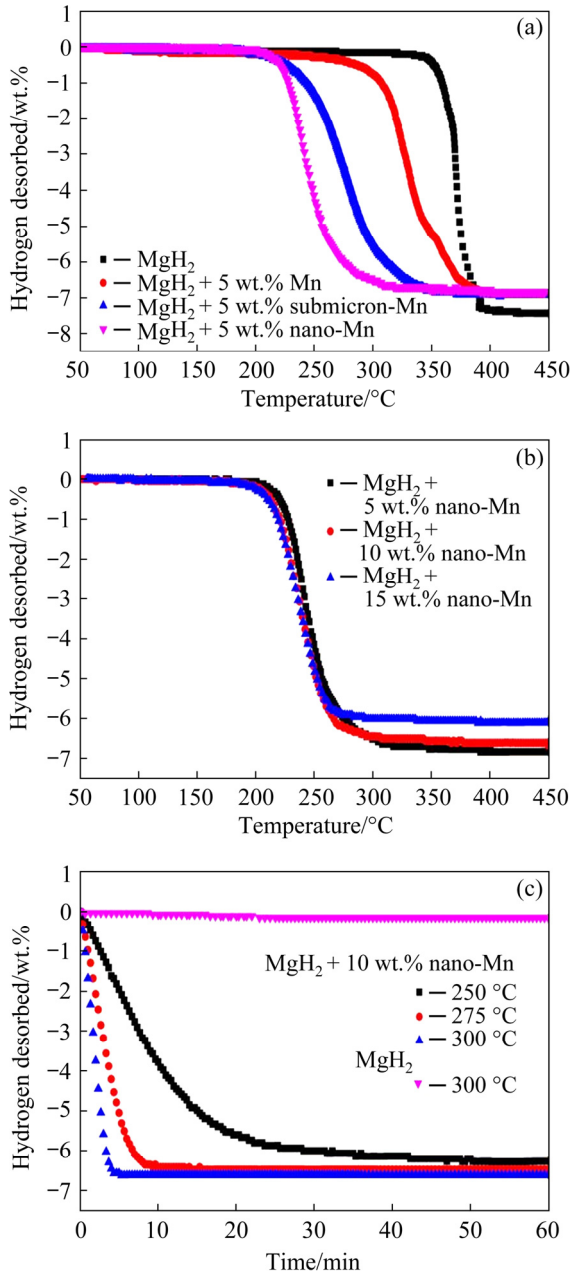


**Fig. 2** Non-isothermal dehydrogenation curves of $MgH_2$ and $MgH_2$ with different Mn [43] (a), non-isothermal dehydrogenation curves of $MgH_2$ + $x$ wt.% nano-Mn ($x$=5, 10, 15) (b) and isothermal dehydrogenation curves of $MgH_2$ and $MgH_2$ + 10 wt.% nano-Mn (c)

amount was increased to 15 wt.%, the dehydrogenation capacity was sharply dropped to 6.0 wt.% due to the dead weight of the catalyst. By considering both the onset dehydrogenation temperature and hydrogen capacity, $MgH_2$ + 10 wt.% nano-Mn was selected for further investigation. Figure 2(c) presents isothermal dehydrogenation curves of $MgH_2$ + 10 wt.% nano-Mn at 250, 275 and 300 °C, respectively. The composite rapidly released 6.7 wt.% hydrogen within 5 min at 300 °C. In addition, $MgH_2$ + 10 wt.% nano-Mn released 6.5 wt.% hydrogen at 275 °C within 10 min and 6.1 wt.% hydrogen at 250 °C within 25 min. As a contrast, additive-free $MgH_2$ could hardly release hydrogen at 300 °C.

The effect of 10 wt.% nano-Mn doping on the hydrogenation process of $MgH_2$ was also investigated. Figure 3(a) shows non-isothermal hydrogenation curves of dehydrogenated $MgH_2$ and $MgH_2$ + 10 wt.% nano-Mn sample. For the fully dehydrogenated $MgH_2$ + 10 wt.% nano-Mn sample, hydrogen up-took was began at room temperature. Rising the temperature to 300 °C, 6.0 wt.% hydrogen could be recharged. However, the completely dehydrogenated $MgH_2$ began to absorb hydrogen from 185 °C, much higher than that of doped sample. Figure 3(b) shows the isothermal hydrogenation curves of dehydrogenated $MgH_2$ + 10 wt.% nano-Mn at 50, 75 and 100 °C under 3 MPa, respectively. It was worth noting that the sample could take up 2.5 and 3.3 wt.% hydrogen at 75 °C and 100 °C in 30 min. Even at low temperature of 50 °C, 2.0 wt.% hydrogen could still be absorbed in 30 min. On the contrary, the isothermal hydrogenation results of $MgH_2$ (Fig. 3(c)) validated that only 2, 3.6 and 5.4 wt.% hydrogen was absorbed in 20 min at 210, 230 and 250 °C, respectively.

The apparent activation energy ($E_a$) of the hydrogen absorption reaction was calculated based on the data of isothermal hydrogenation and Johnson−Mehl−Avrami−Kolmogorov (JMAK) linear equation [45−47]:

$$\ln(-\ln(1-\alpha))=n(\ln k+\ln t) \quad (1)$$

where $\alpha$ represents the mass fraction of Mg converted to $MgH_2$ when the reaction time is $t$, $k$ represents the effective kinetic parameter and $n$ represents the Avrami index. According to the experimental data obtained from isothermal hydrogenation examination, the relationship of $\ln(-\ln(1-\alpha))$ and $\ln t$ can be obtained. Subsequently, $E_a$ of the hydrogen absorption reaction was estimated by Arrhenius equation [41]:

$$k = A\exp\left(-E_a/(RT)\right) \quad (2)$$

where $T$ is isothermal hydrogenation temperature and $A$ represents the pre-exponential factor. The calculated results in Fig. 3(d) show that the dehydrogenation $E_a$ of $MgH_2$ + 10 wt.% nano-Mn

was (18.8±0.2) kJ/mol, which is significantly lower than that of pure $MgH_2$ ((72.5±2.7) kJ/mol, $R^2$=0.997). Therefore, the addition of nano-Mn could effectively reduce the apparent activation energy of hydrogenation reaction, which plays a great role in improving the hydrogenation performance of $MgH_2$. In conclusion, Mn nanoparticles could be served as bidirectional catalysts for improving both the hydrogenation and dehydrogenation properties of $MgH_2$.

### 3.3 Modification mechanism of Mn nanoparticles in hydrogen absorption and desorption

Above experimental results demonstrated the exciting catalytic action of as-prepared Mn towards $MgH_2$, and the modification mechanism needs to be further studied. In order to explore the evolution of nano-Mn in the hydrogenation and dehydrogenation process of $MgH_2$, XRD tests were carried out. As shown in Fig. 4(b), only the phases of Mg and Mn were detected in completely dehydrogenated sample. After hydrogenation, Mg was charged to $MgH_2$ but Mn could still be found in the composite. It could be speculated that Mn did not react with $Mg/MgH_2$ and acted as catalytic union during the hydrogenation and dehydrogenation process.

TEM images of the ball-milled composite are shown in Fig. 5(a), from which it could be seen that the average size of $MgH_2$ + 10 wt.% nano-Mn composite was about 400 nm, while the particle size of $MgH_2$ without catalyst was more than 800 nm. As mentioned above and in the previous report [42], the decrease of particle size was beneficial to improving the hydrogen absorption and desorption properties of $MgH_2$. The diffraction patterns observed in selected area electron diffraction (SAED) patterns belong to $MgH_2$ phase ((400) and (402)) and Mn phase ((622)) separately, agree well with the XRD results, indicating that there was no new phases appearing in the ball milling process. The corresponding EDS spectra with elemental mapping shows that Mn nanoparticles had a close contact with $MgH_2$. By combing the XRD results with TEM analysis, the nano-Mn dispersed on the surface of $MgH_2$ could serve as hydrogen pump site

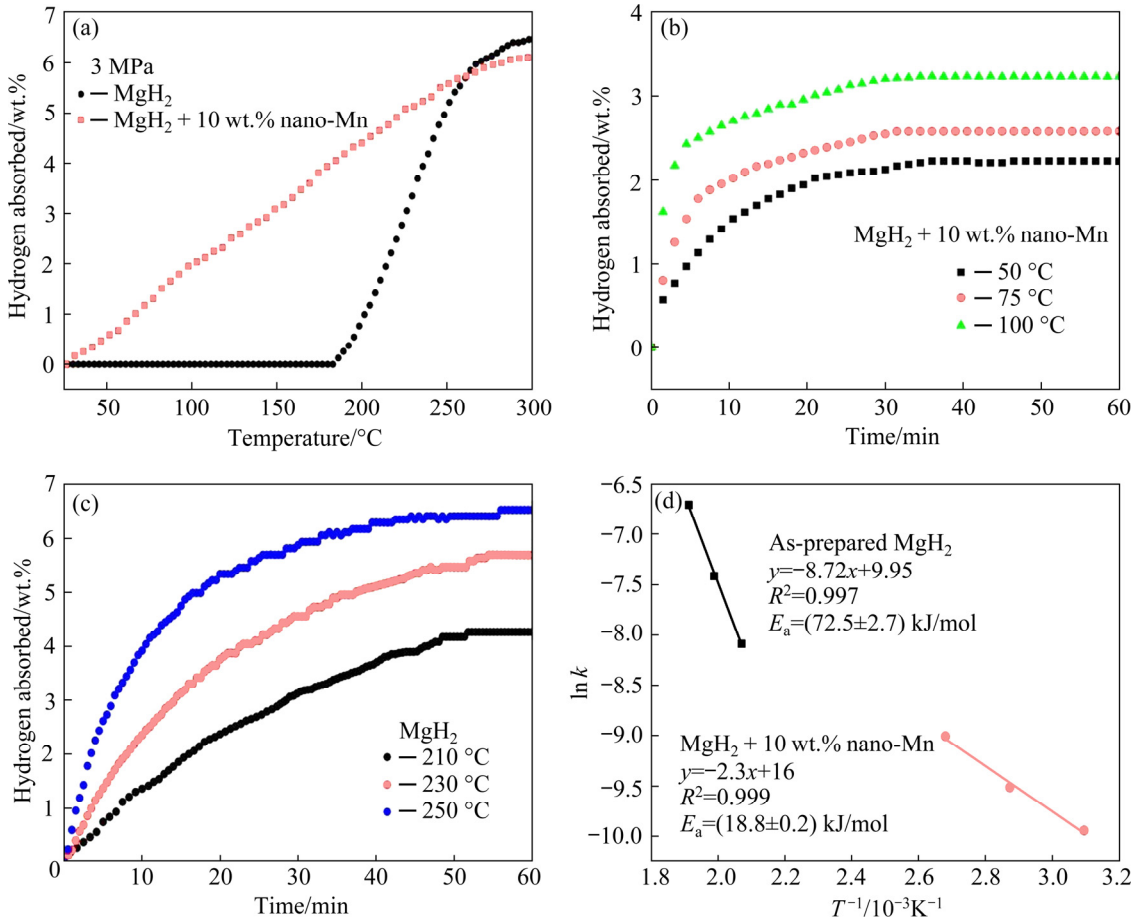


**Fig. 3** Non-isothermal hydrogenation curves (a), isothermal hydrogenation curves at different temperatures (b, c) and corresponding Arrhenius plots (d) of $MgH_2$ with and without 10 wt.% nano-Mn

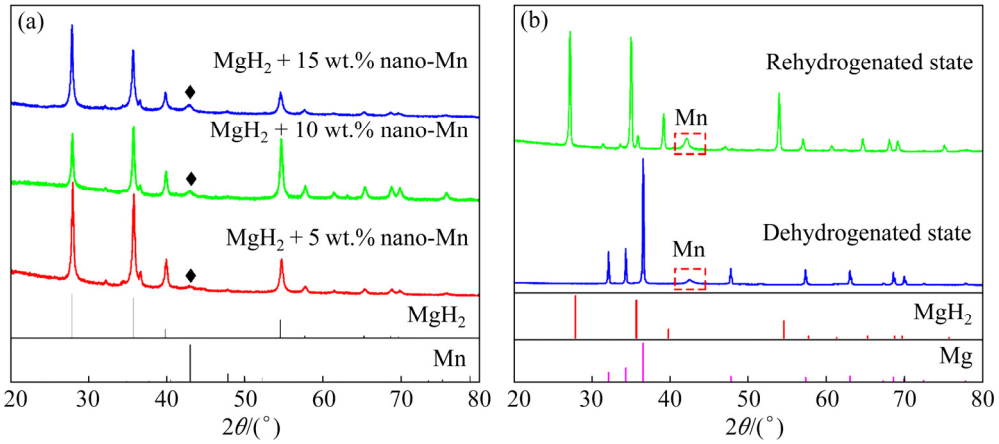


**Fig. 4** XRD patterns of $MgH_2$, $MgH_2$ + 5 wt.% nano-Mn, $MgH_2$ + 10 wt.% nano-Mn and $MgH_2$ + 15 wt.% nano-Mn samples (a), dehydrogenated and rehydrogenated $MgH_2$ + 10 wt.% nano-Mn samples (b)

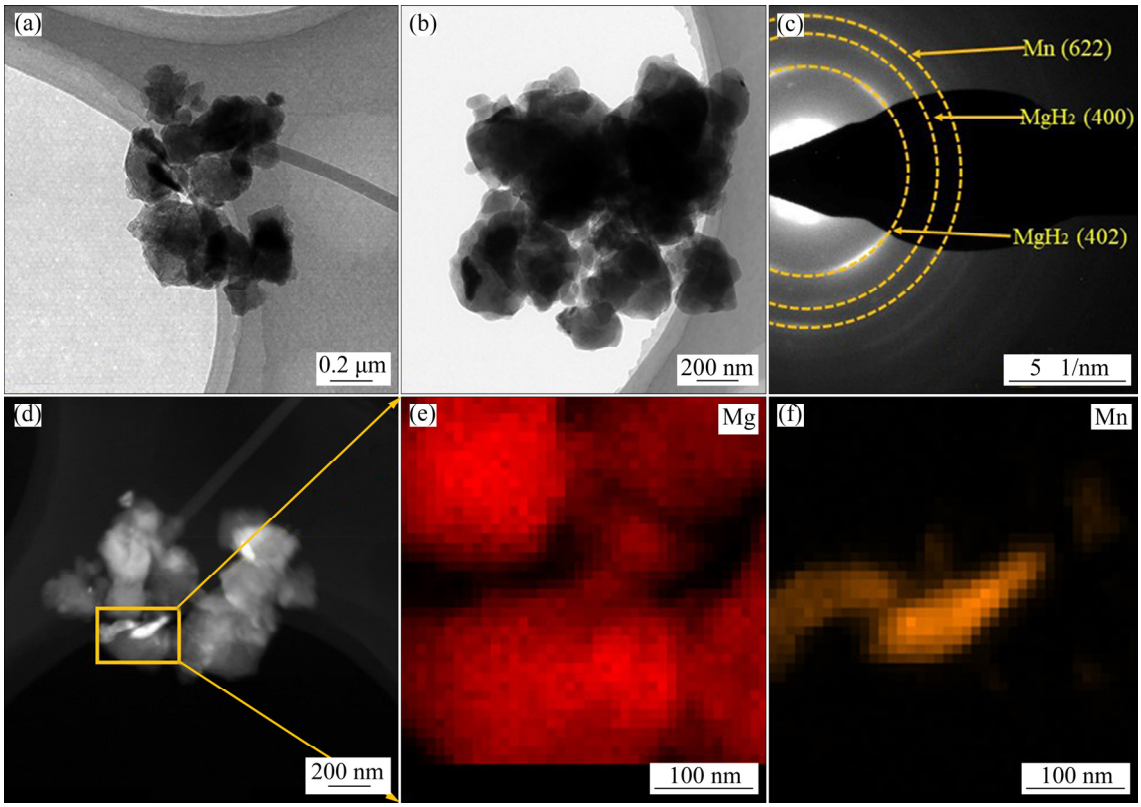


**Fig. 5** TEM photographs (a, b), SAED pattern (c) and corresponding EDS spectra (d) with elemental mapping of Mg (e) and Mn (f) for $MgH_2$ + 10 wt.% nano-Mn composite

to promote the diffusion of hydrogen, thus reducing the reaction energy barrier and improving the dehydrogenation and hydrogenation properties of the $MgH_2$ system.

### 3.4 Cyclic performance of $MgH_2$ + 10 wt.% nano-Mn composite

As an important parameter to evaluate the hydrogen storage performance, cycle stability is also a key factor for the practical application of hydrogen storage materials. Therefore, the $MgH_2$ + 10 wt.% nano-Mn composite was tested for consecutive hydrogenation and dehydrogenation for 20 times at a constant temperature of 275 °C. The hydrogen storage pressure during hydrogenation is 3.2 MPa, and the cyclic hydrogenation and dehydrogenation curves are shown in Fig. 6. For the first hydrogen absorption and desorption process,

the $MgH_2$ + 10 wt.% nano-Mn composite can rapidly release about 6.4 wt.% hydrogen and absorb about 6.2 wt.% hydrogen. After 20 cycles, 5.9 wt.% hydrogen could be released, maintaining 92% of the initial capacity. Compared with the previous research [42], the cycling behavior is better than that of $MgH_2$ + 10 wt.% submicron-Mn sample. At present, many researches [48−51] have shown that there are two main reasons affecting the cycle stability of Mg based hydrogen storage system. One is that the catalysts will be separated from the matrix material during cycling, affecting the subsequent reaction. The other is that the particle size of the matrix material will increase and particles will agglomerate at high temperature. The results presented in this work showed that decreasing the particle size of the catalysts was beneficial to the cycling performance of $MgH_2$, which served as a good inspiration for the further practical application of hydrogen storage materials based on Mg.

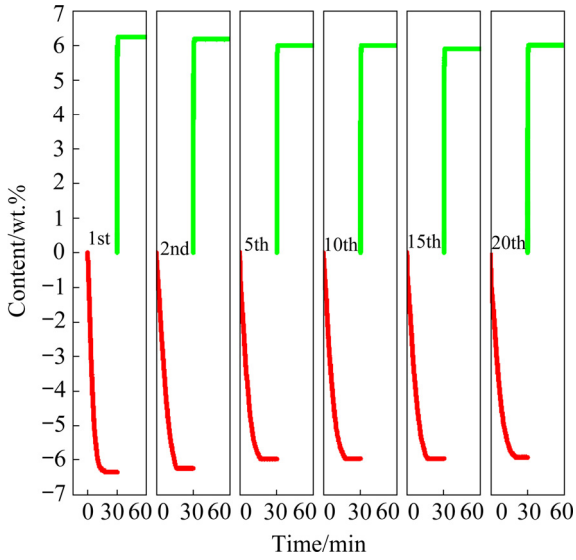


**Fig. 6** Cyclic isothermal dehydrogenation/hydrogenation curves of $MgH_2$ + 10 wt.% nano-Mn sample

## 4 Conclusions

(1) The $MgH_2$ + 10 wt.% nano-Mn began to desorb hydrogen at 175 °C, which was 180 °C lower than that of $MgH_2$. A hydrogen capacity of 6.7 wt.% could be obtained within 5 min at 300 °C.

(2) In hydrogenation, the composite could take up hydrogen at room temperature and 2.0 wt.% hydrogen was charged within 30 min even at the low temperature of 50 °C. The hydrogenation activation energy of $MgH_2$ was reduced from (72.5±2.7) to (18.8±0.2) kJ/mol after doping with 10 wt.% nano-Mn.

(3) The kinetics and hydrogen storage capacity of $MgH_2$ + 10 wt.% nano-Mn composite had no obvious attenuation after 20 hydrogenation and dehydrogenation cycles.

## Acknowledgments

The authors are grateful for the financial supports from the National Natural Science Foundation of China (No. 51801078) and the Natural Science Foundation of Jiangsu Province, China (No. BK20180986).

## References

[1] ABE J O, POPOOLA A, AJENIFUJA E, POPOOLA O M. Hydrogen energy, economy and storage: Review and recommendation [J]. International Journal of Hydrogen Energy, 2019, 44: 15072−15086.

[2] KONG Ling-guo, LI Liang-yuan, CAI Guo-wei, LIU Chuang, MA Ping, BIAN Yu-dong, MA Tao. Techno-economic analysis of hydrogen energy for renewable energy power smoothing [J]. International Journal of Hydrogen Energy, 2020, 46: 2847−2861.

[3] ZHANG Fan, ZHAO Peng-cheng, NIU Meng, MADDY J. The survey of key technologies in hydrogen energy storage [J]. International Journal of Hydrogen Energy, 2016, 41: 14535−14552.

[4] HUO Quan-hui, YANG Xing-lin, ZHANG Jia-qi. Review on hydrogen storage performance of $MgH_2$: Development and trends [J]. ChemistrySelect, 2021, 6: 1589−1606.

[5] BOATENG E, CHEN Ai-cheng. Recent advances in nanomaterial-based solid-state hydrogen storage [J]. Materials Today Advances, 2020, 6: 100022.

[6] LE T T, PISTIDDA C, NGUYEN V H, SINGH P, RAIZADA P, KIASSEN T, DORNHEIM M. Nanoconfinement effects on hydrogen storage properties of $MgH_2$ and $LiBH_4$ [J]. International Journal of Hydrogen Energy, 2021, 46: 23723−23736.

[7] EL-ESKANDARANY M S. Recent developments in the fabrication, characterization and implementation of $MgH_2$-based solid-hydrogen materials in the Kuwait Institute for Scientific Research [J]. RSC Advances, 2019, 9: 9907−9930.

[8] ZHENG Jin-yang, LIU Xian-xin, XU Ping, LIU Peng-fei, ZHAO Yong-zhi, YANG Jian. Development of high pressure gaseous hydrogen storage technologies [J]. International Journal of Hydrogen Energy, 2012, 37: 1048−1057.

[9] SHAO Huai-yu, HE Li-qing, LIN Huai-jun, LI Hai-wen. Progress and trends in magnesium-based materials for energy-storage research: A review [J]. Energy Technology Generation Conversion Storage Distribution, 2018, 6: 445−458.

[10] LIU Xiao-sheng, LIU Hai-zhen, QIU Ning, ZHANG Yan-bing, ZHAO Guang-yao, XU Li, LAN Zhi-qiang, GUO Jin. Cycling hydrogen desorption properties and microstructures

of $MgH_2$−$AlH_3$−$NbF_5$ hydrogen storage materials [J]. Rare Metals, 2021, 40: 1003−1007.

[11] SHANG Yuan-yuan, PISTIDDA C, GIZER G, KLASSEN T, DORNHEIM M. Mg-based materials for hydrogen storage [J]. Journal of Magnesium and Alloys, 2021. https://doi.org/10.1016/j.jma.2021.06.007

[12] DORNHEIM M, DOPPIU S, BARKHORDARIAN G, BOESENBERG U, KLASSEN T, GUTFLEISCH O, BORMANN R. Hydrogen storage in magnesium-based hydrides and hydride composites [J]. Scripta Materialia, 2007, 56: 841−846.

[13] YARTYS V A, LOTOTSKYY M V, AKIBA E, ALBERT R, ANTONOV V E, ARES J R, BARICCO M, BOURGEOIS N, BUCKLEY C E, BELLOSTA V. Magnesium based materials for hydrogen based energy storage: Past, present and future [J]. International Journal of Hydrogen Energy, 2019, 44: 7809−7859.

[14] CRIVELLO J C, DAM B, DENYS R V, DORNHEIM M, GRANT D M, HUOT J, JENSEN T R, de JONGH P, LATROCHE M, MILANESE C, MILCIUS D, WALKER G S, WEBB C J, ZLOTEA C, YARTYS V A. Review of magnesium hydride-based materials: Development and optimisation [J]. Applied Physics A, 2016, 122: 97.

[15] CHAWLA K, YADAV D K, BAJPAI A, KUMAR S, LAL C. Hydrogenation properties and kinetic study of $MgH_2$−$x$wt.% AC nanocomposites prepared by ball milling [J]. Environmental Science and Pollution Research, 2021, 28: 3872−3879.

[16] BARDHAN R, RUMINSKI A M, BRAND A, URBAN J J. Magnesium nanocrystal−polymer composites: A new platform for designer hydrogen storage materials [J]. Energy & Environmental Science, 2011, 4: 4882−4895.

[17] RIZO-ACOSTA P, CUEVAS F, LATROCHE M. Optimization of $TiH_2$ content for fast and efficient hydrogen cycling of $MgH_2$−$TiH_2$ nanocomposites [J]. International Journal of Hydrogen Energy, 2018, 43: 16774−16781.

[18] SHEVLIN S A, GUO Zheng-xiao. $MgH_2$ dehydrogenation thermodynamics: Nanostructuring and transition metal doping [J]. The Journal of Physical Chemistry C, 2013, 117: 10883−10891.

[19] ZHANG Liu-ting, JI Liang, YAO Zhen-dong, YAN Nian-hua, SUN Ze, YANG Xing-lin, ZHU Xin-qiao, HU Shuang-lin, CHEN Li-xin. Facile synthesized Fe nanosheets as superior active catalyst for hydrogen storage in $MgH_2$ [J]. International Journal of Hydrogen Energy, 2019, 44: 21955−21964.

[20] LU Chong, MA Yan-ling, LI Fan, ZHU Hong, MENG Fan-qi, DING Wen-jiang, WU Jian-bo, DENG Tao, ZOU Jian-xin. Visualization of fast "hydrogen pump" in core–shell nanostructured Mg@Pt through hydrogen-stabilized $Mg_3Pt$ [J]. Journal of Materials Chemistry A, 2019, 7: 2050−7496.

[21] LU Yan-shan, KIM H, SAKAKI K, HAYASHI S, JIMURA K, ASANO K. Destabilizing the dehydrogenation thermodynamics of magnesium hydride by utilizing the immiscibility of Mn with Mg [J]. Inorganic Chemistry, 2019, 58: 14600−14607.

[22] ZHOU Dian-wu, PENG Ping, LIU Jin-shui, CHEN Lu, HU Yan-jun. First-principles study on structural stability of 3d transition metal alloying magnesium hydride [J]. Transactions of Nonferrous Metals Society of China, 2006, 16: 23−32.

[23] YONG Hui, GUO Shi-hai, YUAN Ze-ming, QI Yan, ZHAO Dong-liang, ZHANG Yang-huan. Phase transformation, thermodynamics and kinetics property of $Mg_{90}Ce_5RE_5$ (RE= La, Ce, Nd) hydrogen storage alloys [J]. Journal of Materials Science and Technology, 2020, 51: 84−93.

[24] FENG Dian-chen, SUN Hao, WANG Xi-tao, ZHANG Yang-huan. Effect of milling duration on hydrogen storage thermodynamics and kinetics of ball-milled Ce−Mg−Ni-based alloy powders [J]. Journal of Iron and Steel Research International, 2018, 25: 746−754.

[25] LI Zhen-yang, LI Sheng-li, YUAN Ze-ming, ZHANG Yang-huan, QI Yan. Microstructure, hydrogen storage thermodynamics and kinetics of $La_5Mg_{95-x}Ni_x$ ($x$=5, 10, 15) alloys [J]. Transactions of Nonferrous Metals Society of China, 2019, 29: 1057−1066.

[26] KONG Qian-qian, ZHANG Huan-huan, YUAN Zhen-luo, LIU Jia-meng. Hamamelis-like $K_2Ti_6O_{13}$ synthesized by alkali treatment of $Ti_3C_2$ MXene: Catalysis for hydrogen storage in $MgH_2$ [J]. ACS Sustainable Chemistry & Engineering, 2020, 8: 4755−4763.

[27] MA Zhe-wen, ZOU Jian-xin, KHAN D, ZHU Wen, HU Chuan-zhu, ZENG Xiao-qin, DING Wen-jiang. Preparation and hydrogen storage properties of $MgH_2$-trimesic acid-TM MOF (TM=Co, Fe) composites [J]. Journal of Materials Science & Technology, 2019, 35: 2132−2143.

[28] OELERICH W, KLASSEN T, BORMANN R. Metal oxides as catalysts for improved hydrogen sorption in nanocrystalline Mg-based materials [J]. Journal of Alloys and Compounds, 2001, 315: 237−242.

[29] PENG Shu-ke, XIAO Xue-zhang, XU Rui-juan, LI Luo, WU Fan, LI Shuo-quan, WANG Qi-dong, CHEN Li-xin. Hydrogen storage behaviors and microstructure of $MF_3$ (M=Ti, Fe)-doped magnesium hydride [J]. Transactions of Nonferrous Metals Society of China, 2020, 20: 1879−1884.

[30] ZHONG Hai-chang, XU Jing-bo, JIANG Chun-hai, LU Xiang-jun. Microstructure and remarkably improved hydrogen storage properties of $Mg_2Ni$ alloys doped with metal elements of Al [J]. Transactions of Nonferrous Metals Society of China, 2018, 28: 2470−2477.

[31] SUN Ze, LU Xiong, NYAHUMA F M, YAN Nian-hua, XIAO Jian-kun, SU Shi-chuan, ZHANG Liu-ting. Enhancing hydrogen storage properties of $MgH_2$ by transition metals and carbon materials: A brief review [J]. Frontiers in Chemistry, 2020, 8: 522.

[32] ZHANG Meng, XIAO Xue-zhang, LUO Bo-sang, LIU Mei-jia, CHEN Man, CHEN Li-xin. Superior de/hydrogenation performances of $MgH_2$ catalyzed by 3D flower-like $TiO_2$@C nanostructures [J]. Journal of Energy Chemistry, 2019, 46: 191−198.

[33] WANG Ze-yi, ZGANG Xue-liang, REN Zhuang-he, LIU Yong, HU Jian-jiang, LI Hai-wen, GAO Ming-xia, PAN Hong-ge, LIU Yong-feng. In situ formed ultrafine NbTi nanocrystals from a NbTiC solid-solution MXene for hydrogen storage in $MgH_2$ [J]. Journal of Materials Chemistry A, 2019, 7: 14244−14252.

[34] CHENG Hong-hui, CHEN Gang, ZHANG Yao, ZHU Yun-feng, LI Li-quan. Boosting low-temperature de/re-hydrogenation performances of $MgH_2$ with Pd−Ni bimetallic nanoparticles supported by mesoporous carbon [J]. International Journal of Hydrogen Energy, 2019, 44: 10777−10787.

[35] PLUENGPHON P, BOVORNRATANARAKS T, TAUPPAYAKORN-AEK P, PINSOOK U, INCEESUNGVORN B. High-pressure phases induce H-vacancy diffusion kinetics in TM-doped $MgH_2$: Ab initio study for hydrogen storage improvement [J]. International Journal of Hydrogen Energy, 2019, 44: 21948−21954.

[36] SUN Gai-li, LI Yuan-yuan, ZHAO Xin-xin, WU Jian-bao, MI Yi-ming, WANG Li-li. First-principles investigation of effects of Ni and Y co-doped on destabilized $MgH_2$ [J]. RSC Advances, 2016, 6: 23110−23116.

[37] LIANG Guo-xian, HUOT J, BOILY S, van NESTE A, SCHULZ R. Catalytic effect of transition metals on hydrogen sorption in nanocrystalline ball milled $MgH_2$−Tm (Tm=Ti, V, Mn, Fe and Ni) systems [J]. Journal of Alloys and Compounds, 1999, 292: 247−252.

[38] ZHANG Liu-ting, LU Xiong, JI Liang, YAN, Nian-hua, SUN Ze, ZHU Xin-qiao. Catalytic effect of facile synthesized TiH1.971 nanoparticles on the hydrogen storage properties of $MgH_2$ [J]. Nanomaterials, 2019, 9: 1370.

[39] MA Zhong-liang, ZHANG Ji-guang, ZHU Yun-feng, LIU Ya-na, ZHANG Yao, ZHU De-long, LI Li-quan. Facile synthesis of carbon supported nano-Ni particles with superior catalytic effect on hydrogen storage kinetics of $MgH_2$ [J]. ACS Applied Energy Materials, 2018, 1: 1158−1165.

[40] PATELLI N, CALIZZI M, MIGLIORI A, MORANDI V, PASQUINI L. Hydrogen desorption below 150 °C in $MgH_2$−$TiH_2$ composite nanoparticles: Equilibrium and kinetic properties [J]. Journal of Physical Chemistry, C, 2017, 121: 11166−11177.

[41] ZHANG Liu-ting, CAI Ze-liang, YAO Zhen-dong, JI Liang, SUN Ze, YAN Nian-hua, ZHANG Bei-yu, XIAO Bei-bei, DU Jun, ZHU Xin-qiao, CHEN Li-xin. A striking catalytic effect of facile synthesized $ZrMn_2$ nanoparticles on the de/rehydrogenation properties of $MgH_2$ [J]. Journal of Materials Chemistry A, 2019, 7: 5626−5634.

[42] SUN Ze, ZHANG Liu-ting, YAN Nian-hua, ZHENG Jia-guang, BIAN Ting, YANG Zong-ming, SU Shi-chuan. Realizing hydrogen de/absorption under low temperature for $MgH_2$ by doping Mn based catalysts [J]. Nanomaterials, 2020, 10: 1745.

[43] TIAN Mi, SHANG Cong-xiao. Nano-structured $MgH_2$ catalyzed by TiC nanoparticles for hydrogen storage [J]. Journal of Chemical Technology & Biotechnology, 2011, 86: 69−74.

[44] BHAT V V, ROUGIER A, AYMARD L, NAZRI G A, TARASCON J M. High surface area niobium oxides as catalysts for improved hydrogen sorption properties of ball milled $MgH_2$ [J]. Journal of Alloys and Compounds, 2008, 460: 507−512.

[45] AVRAMI M. Kinetics of phase change. I: General theory [J]. Journal of Chemical Physics, 1939, 8: 1103−1112.

[46] ADAM S, JONAS A, THOMAS K N, YNGVE C, TORBEN R, MARTIN S. Hydrogen absorption and desorption properties of a novel ScNiAl alloy [J]. Applied Physics A, 2011, 104: 235−238.

[47] GAO Shi-chao, WANG Xin-hua, LIU Hai-zhen, HE Ting, WANG Yuan-yuan, LI Shou-quan, YAN Mi. Effects of nano-composites (FeB, FeB/CNTs) on hydrogen storage properties of $MgH_2$ [J]. Journal of Power Sources, 2019, 438: 227006.

[48] LIU Mei-jia, XIAO Xue-zhang, ZHAO Shu-chun, SINASAREMI-YARAHMADIC S, CHEN Man, ZHENG Jia-guang, LI Shuo-quan, CHEN Li-xin. ZIF-67 derived Co@CNTs nanoparticles: Remarkably improved hydrogen storage properties of $MgH_2$ and synergetic catalysis mechanism [J]. International Journal of Hydrogen Energy, 2019, 44: 1059−1069.

[49] SADHASIVAM T, KIM H T, JUNG S, ROH S H, PARK J H, JUNG H Y. Dimensional effects of nanostructured Mg/$MgH_2$ for hydrogen storage applications: a review [J]. Renewable & Sustainable Energy Reviews, 2017, 72: 523−534.

[50] LI Yang, LI Ping, TAN Qi-wei, ZHANG Zong-liang, WAN Qi, LIU Zhi-wei, SUBRAMANIAN A, QU Huan-hui. Thermal properties and cycling performance of $Ca(BH_4)_2$/$MgH_2$ composite for energy storage [J]. Chemical Physics Letters, 2018, 700: 44−49.

[51] UTKE R, PLERDSRANOY P. Ternary $LiBH_4$−$MgH_2$−$NaAlH_4$ hydride confined into nanoporous carbon host for reversible hydrogen storage [J]. Journal of Physics & Chemistry of Solids, 2016, 90: 80−86.

# Mn 纳米颗粒增强 $MgH_2$ 的吸放氢动力学

陈 艳[1]，章浩宇[1]，吴富英[2]，孙 泽[1]，郑家广[1]，张刘挺[1]，陈立新[3]

1. 江苏科技大学 能源与动力学院，镇江 212003；2. 江苏科技大学 分析测试中心，镇江 212003；
3. 浙江大学 材料科学与工程系 硅材料国家重点实验室，杭州 310027

**摘 要：**合成锰纳米颗粒并掺杂到 $MgH_2$ 中以改善其吸放氢性能。与 $MgH_2$ 相比，含 10%(质量分数)锰纳米颗粒的 $MgH_2$ 其初始放氢温度下降到 175 °C。在 300、275 和 250 °C 下，该复合体系能在 5、10 和 25 min 之内分别释放出 6.7%、6.5%和 6.1%(质量分数)的氢气。此外，该复合体系在室温下即可吸氢，并能在 50 °C、30 min 之内吸收 2.0%(质量分数)的氢气。在掺杂 10%(质量分数)锰纳米颗粒后，$MgH_2$ 吸氢反应的活化能从(72.5±2.7) kJ/mol 降低到(18.8±0.2) kJ/mol，该复合体系表现出优异的循环性能，在 20 次循环后保持着 92%的初始容量。

**关键词：**储氢材料；氢化镁；锰纳米颗粒；催化机理；可逆性

**(Edited by Bing YANG)**